Semiclassical angular scattering in the F+H−2 −> HF+Hreaction: Regge pole analysis using the Pade approximation

ARTICLE *in* CHEMICAL PHYSICS LETTERS · NOVEMBER 1999

Impact Factor: 1.9 · DOI: 10.1016/S0009-2614(99)01016-7

3 AUTHORS, INCLUDING:

D. Sokolovski
Universidad del País Vasco / Euskal H…
108 PUBLICATIONS **1,112** CITATIONS
SEE PROFILE

Jesus F Castillo
Complutense University of Madrid
76 PUBLICATIONS **2,064** CITATIONS
SEE PROFILE

5 November 1999

ELSEVIER

Chemical Physics Letters 313 (1999) 225–234

CHEMICAL PHYSICS LETTERS

www.elsevier.nl/locate/cplett

Semiclassical angular scattering in the $F + H_2 \rightarrow HF + H$ reaction: Regge pole analysis using the Padé approximation

D. Sokolovski [a,*], J.F. Castillo [b], C. Tully [a]

[a] *Theoretical and Computational Physics Research Division, Department of Applied Mathematics and Theoretical Physics, Queen's University of Belfast, Belfast BT7 1NN, UK*

[b] *Departamento de Quimica Fisica I, Universidad Complutense de Madrid, Madrid 28040, Spain*

Received 22 March 1999; in final form 24 May 1999

Abstract

We apply the complex angular momentum analysis to study state-selective forward scattering in the $F + H_2$ reaction. The scattering matrix calculated by Castillo et al. is used. The S-matrix element is analytically continued into the complex plane of the total angular momentum with the help of the Padé approximation. Resonance (Regge) poles are identified and their residues evaluated. The semiclassical optical model is corrected to account for finite lifeangles of leading resonances. For chosen transitions, the forward scattering enhancement is shown to be a resonance effect due to the decay of a Regge state with angular life of about 32°. © 1999 Elsevier Science B.V. All rights reserved.

1. Introduction

Reactive angular distributions in the $F + H_2 \rightarrow FH + H$ reaction have been a subject of much attention for more than a decade [1–5]. Their main feature, the state-selective forward angle scattering, was observed by Neumark and co-workers in 1985 [1]. Neumark et al. suggested that the enhanced forward scattering for $HF(v' = 3)$ was due to the existence of a long-lived state formed during the reaction [1]. However, quasiclassical trajectory studies on the Stark–Werner (SW) potential energy surface (PES) [2] have demonstrated that classical trajectories producing $HF(v' = 3)$ also have a tendency to be scattered in the forward direction, thus suggesting a different explanation for the effect. Quantum-mechanical calculations on the SW PES [3,4] showed even greater forward scattering. Whether enhanced forward scattering in $F + H_2$ has a direct or resonance origin remained an open question.

The authors of Ref. [3] analysed time delays associated with the peak structure in the cumulative reaction probability at zero total angular momentum J versus energy E and concluded that no long-lived state was involved. An additional observation was made by Dobbyn et al. [5]. They have pointed out that, for a light system, the angular life of a resonance can be considerable even if the complex is relatively short-lived. It was also demonstrated that the direct scattering optical model of Herschbach [6] fails to reproduce correctly the small angle scattering for $F + H_2 \rightarrow FH + H$. Using a more sophisticated nearside–farside analysis [6] the authors of Ref. [5] suggested that the oscillatory structures in the angular distributions were consistent with the presence of

* Corresponding author. Fax: +44-1232-239-182; e-mail: d.sokolovski@qub.ac.uk

0009-2614/99/$ - see front matter
PII: S0009-2614(99)01016-7

a single Regge state with a lifeangle of 30°–40° at a total energy $E = 0.4309$ eV. A more rigorous analysis of the problem is required [5].

In this Letter, we present a detailed analysis of resonance contributions to the zero helicity state-to-state differential cross-sections obtained in quantum calculations [4]. In a slightly modified form, we shall apply the semiclassical theory of resonance angular scattering developed in Refs. [7,8]. This Letter is organised as follows: in Section 2, we apply the Poisson sum formula to obtain an integral representation for the reactive scattering amplitude. In Section 3, we use the Padé approximation to analytically continue the S-matrix elements into the complex plane of the total angular momentum and identify the resonance poles. In Section 4, we use the Padé approximation to construct a semiclassical optical model similar to that of Herschbach [6]. This model will fail if resonances with large lifeangles are present. In Section 5, we define the lifetime correction function (LCF) to correct the optical model. In Section 6, we give the results for the $F + H_2 \rightarrow FH + H$ reactions. Section 7 contains our conclusions.

2. Reactive scattering amplitude

For an atom–diatom collision, $A + BC \rightarrow AB + C$ the reactive scattering amplitude $f_{\nu' \leftarrow \nu}$ is given by the partial wave series [9,10],

$$f_{\nu' \leftarrow \nu}(\theta) = (ik_\nu)^{-1} \sum_{J=J_{\min}}^{\infty} (J+1/2)\, d^J_{M'M}(\theta) S^J_{\nu' \leftarrow \nu}, \tag{1.1}$$

where $\nu, (\nu')$ is a collective index, $\nu \equiv (\upsilon, j, M)$, comprising the vibrational and rotational quantum numbers of the molecule, υ and j, and the momentum (p-) helicity M (projection of the molecule's angular momentum onto the atom–molecule relative velocity). In addition, J is the total angular momentum quantum number, θ is the centre of mass scattering angle (Fig. 1), k_ν is the translational wavevector in the incident channel and $J_{\min} \equiv \max(|M|,|M'|)$. If both helicities are zero, $M = M' = 0$, the Wigner matrices $d^J_{M'M}(\theta)$ [11] reduce to the Legendre polynomials P_J,

$$d^J_{00}(\theta) = P_J(\cos\theta). \tag{1.2}$$

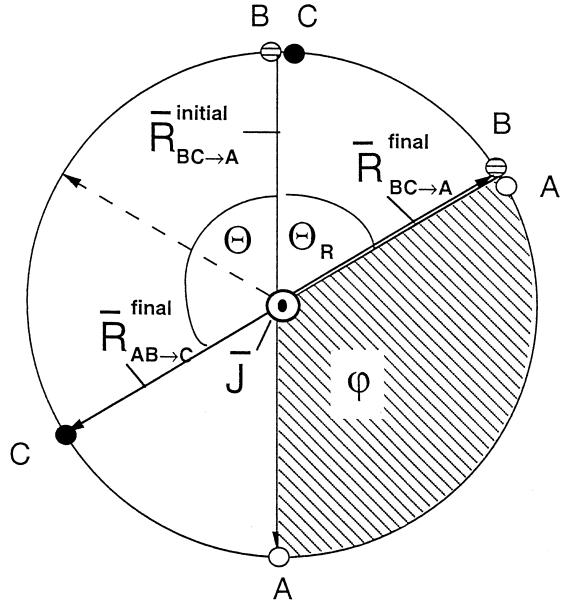

Fig. 1. Initial and final orientations of the inelastic Jacobi vector $\boldsymbol{R}_{BC \rightarrow A}$ and the final direction of the reactive Jacobi vector $\boldsymbol{R}_{AB \rightarrow C}$. The total angular momentum $\boldsymbol{J}$ is perpendicular to the plane of the drawing. In the course of collision $\boldsymbol{R}_{BC \rightarrow A}$ sweeps the angle φ (shaded). Another final direction of $\boldsymbol{R}_{AB \rightarrow C}$, leading to the same scattering angle θ ($\varphi = \pi + \theta$) is shown by a dashed line. Also shown is the reactive scattering angle θ_R.

Using the semiclassical asymptote of $P_J(\cos\theta)$ for large J [12]

$$P_J(\cos\theta) \approx \left[\frac{2}{(J+1/2)\pi \sin\theta}\right]^{1/2} \times \cos\left[(J+1/2)\theta - \pi/4\right], \tag{1.3}$$

$$1/J < \theta < \pi - 1/J.$$

and applying the Poisson sum formula [12] to Eqs. (1.1) and (1.2) we can rewrite the scattering amplitude $f_{\nu' \leftarrow \nu}(\theta)$ in an equivalent form

$$f_{\nu' \leftarrow \nu}(\theta) \approx (ik_i)^{-1}(2\pi \sin\theta)^{-1/2} \times \sum_{k=-\infty}^{\infty} \tilde{f}_{\nu' \leftarrow \nu}(\varphi_k) \exp(-i\pi/4 - ik\pi/2) \tag{1.4}$$

where

$$\tilde{f}_{\nu' \leftarrow \nu}(\varphi) \equiv \int_0^\infty \exp(i\lambda\varphi) S_{\upsilon' \leftarrow \upsilon}(\lambda) \lambda^{1/2}\, d\lambda, \quad -\infty < \varphi < \infty,$$

$$S_{\nu' \leftarrow \nu}(J+1/2) = S^J_{\nu' \leftarrow \nu}, \tag{1.5}$$

and

$$\varphi_k(\theta) = (-1)^k\theta + \pi\left\{k + \left[1-(-1)^k\right]/2\right\},$$
$$\pi k < \varphi_k < \pi(k+1). \qquad (1.6)$$

We shall use representation (1.4)–(1.6) to study resonance effects in reactive angular distributions. Semiclassically, the variable φ in Eq. (1.5) coincides [13] with the angle by which the Jacobi vector $\boldsymbol{R}_{\mathrm{BC}\to\mathrm{A}}$ (i.e. the vector connecting the centre of mass of BC with A) rotates during the collision around the fixed total angular momentum $\boldsymbol{J}$ (Fig. 1) and $\tilde{f}_{\nu'\leftarrow\nu}(\varphi)$ is proportional to the probability amplitude for $\boldsymbol{R}_{\mathrm{BC}\to\mathrm{A}}$ to rotate by φ. How far $\boldsymbol{R}_{\mathrm{BC}\to\mathrm{A}}$ will precess around $\boldsymbol{J}$ depends on the reaction mechanism. If the forces between collision partners are mostly repulsive, direct reactive classical trajectories have $0<\varphi<\pi$ and $\tilde{f}_{\nu'\leftarrow\nu}(\varphi)$ is likely to be contained between $\varphi=0$ and $\varphi=\pi$. If, on the other hand, the atoms form a long-lived intermediate state, rotation of the decaying complex (required to maintain the total angular momentum J) may carry $\boldsymbol{R}_{\mathrm{BC}\to\mathrm{A}}$ to larger φs, and $\tilde{f}_{\nu'\leftarrow\nu}(\varphi)$ would extend beyond the $[0,\pi]$ region. Since the full scattering amplitude (1.4) is obtained by adding, with appropriate phases, contributions from all rotation angles consistent with the scattering angle θ (these are given by Eq. (1.6)) we expect resonances with sufficiently large lifeangles lead to observable interference effects in reactive angular distributions [7,8].

Next we shall use Eqs. (1.4), (1.5) and (1.6) to investigate the origin of forward scattering of the zero-helicity ($M=M'=0$) state-to-state angular distributions of the $\mathrm{F}+\mathrm{H}_2\to\mathrm{FH}+\mathrm{H}$ reaction observed in calculations [3].

3. Padé approximation for the S-matrix. Resonance Regge poles

Usually, a compute code evaluates the S-matrix elements $S^J_{\nu'\leftarrow\nu}$, for integer values of J, $J=0,1,2,3\ldots N$. To reconstruct from this discrete set of values an analytic function $S_{\nu'\leftarrow\nu'}(\lambda)$ in Eq. (1.5), we shall use the Padé approximation [14,15]. We note first that, for a heavy system, the S-matrix element is likely to have a phase which rapidly varies with λ. To avoid reproducing these rapid oscillations we write

$$S_{\nu'\leftarrow\nu}(\lambda) = \exp\left[i\phi(\lambda)\right] s_{\nu'\leftarrow\nu}(\lambda) \qquad (2.1)$$

where $\phi(\lambda)$ is a known analytical function chosen so that remaining $s_{\nu'\leftarrow\nu}(\lambda)$ varies with λ sufficiently slowly. For $s_{\nu'\leftarrow\nu'}(\lambda)$ we have a Padé approximation

$$s_{\nu'\leftarrow\nu}(\lambda) = \sum_{i=1}^{d}\frac{\rho_i}{\lambda-\lambda_i} \equiv \frac{P_{d-1}(\lambda)}{Q_d(\lambda)} \qquad (2.2)$$

where $P_{d-1}(\lambda)$ and $Q_d(\lambda)$ are polynomials of λ of order $d-1$ and d, respectively. A detailed description of the Padé method was given by Bessis et al. in Ref. [15] and, to avoid repetition, we shall only review the procedure briefly. Choosing $2d$ half-integer values $\lambda^{(k)}$, $k=1,2,\ldots,2d\leqslant N$ and using Eqs. (2.1) and (2.2) yields $2d$ equations for $2d$ unknowns ρ_i and λ_i, $i=1,d$

$$S_{\upsilon'\leftarrow\upsilon}(\lambda^{(k)})\exp\left[-i\phi(\lambda^{(k)})\right] = \sum_{i=1}^{d}\frac{\rho_i}{\lambda^{(k)}-\lambda_i},$$
$$k=1,2,\ldots 2d. \qquad (2.3)$$

The non-linear Eq. (2.2) can be solved by expressing the function in the r.h.s as a continued fraction [14]. This allows for determination of the coefficients of the polynomials $P_{d-1}(\lambda)$ and $Q_d(\lambda)$ in Eq. (2.2) and, finally, of the quantities ρ_i and λ_i. Note that a successful Padé approximant should not have any sharp features between the grid points $\lambda^{(k)}$. Also, all physical resonance poles should lie in the first quadrant of the complex λ-plane. Under these conditions Eqs. (2.1) and (2.2) provide an analytic continuation of the S-matrix element in the vicinity of the real λ-axis.

Poles of the S-matrix close to the real axis correspond to metastable states of the triatomic [7,8]. Separating in Eq. (2.3) those, say, N_{res} ($N_{\mathrm{res}}<d$) poles which correspond to the resonances from those which contribute to the smooth 'background' $q(\lambda)$, we have

$$S_{\nu'\leftarrow\nu}(\lambda) = \exp\left[i\phi(\lambda)\right]\left\{\sum_{m=1}^{N_{\mathrm{res}}}\frac{\rho_m}{\lambda-\lambda_m} + q(\lambda)\right\} \qquad (2.4)$$

where $q(\lambda)$ includes all remaining terms in Eq. (2.3). The resonance poles in Eq. (2.4) may be chosen to ensure that the remaining $q(\lambda)$ has as little structure as possible.

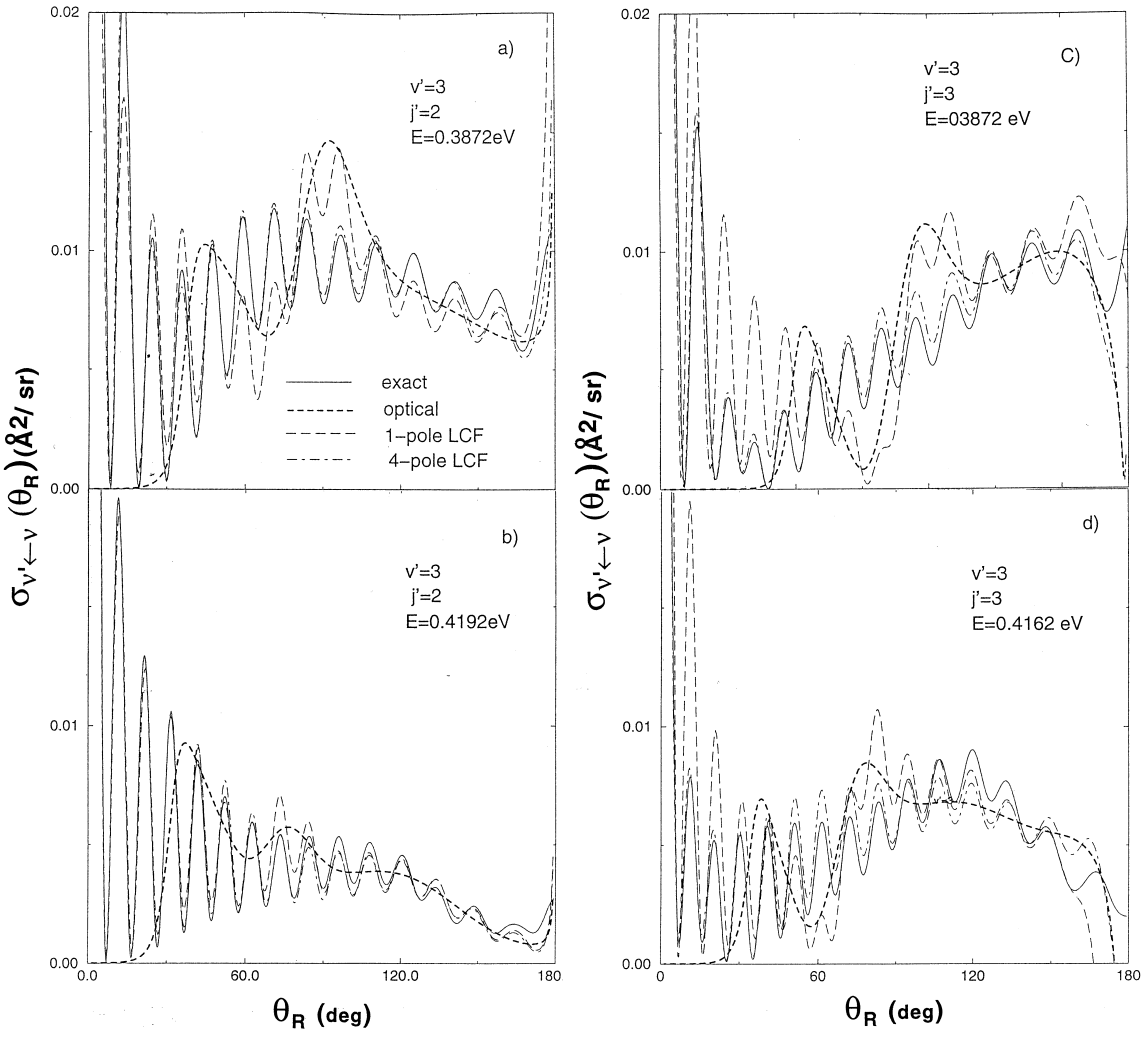

Fig. 2. (a) Differential cross-sections for the (3,2,0) ← (0,0,0) transition at $E = 0.3872$ eV vs. $\theta_R = \pi - \theta$: exact PWS Eq. (1.1) (solid); optical model Eq. (3.5) (short dash); corrected optical model Eq. (4.9) with only $m = 1$ pole in Table 1 included in the LCF (long dash), corrected optical model Eq. (4.9) with $m = 1,2,3,4$ poles in Table 1 included in the LCF (dot-dash). (b) Same as (a) but for the (3,2,0) ← (0,0,0) transition at $E = 0.4162$ eV. (c) Same as (a) but for the (3,3,0) ← (0,0,0) transition at $E = 0.3872$ eV. (d) Same as (a) but for the (3,3,0) ← (0,0,0) transition at $E = 0.4162$ eV.

In this Letter, we shall analyse two transitions (details of the calculation can be found in Ref. [4]), for which the angular distributions show considerable amount of forward scattering (Fig. 2)

$$v' = 3,\ j' = 2,\ M' = 0 \leftarrow v = 0,\ j = 0,\ M = 0, \tag{2.5a}$$

$$v' = 3,\ j' = 3,\ M' = 0 \leftarrow v = 0,\ j = 0,\ M = 0 \tag{2.5b}$$

at two higher total energies corresponding to the collision energies in the Neumark et al. experiment [1], $E_1 = 0.3872$ eV and $E_2 = 0.4162$ eV. The four differential cross-sections in Fig. 2 require up to 26 partial waves to converge, $N = 26$, and in Eq. (2.2) we have $d < 13$. In each case, we have used a quadratic approximation for the phase in Eq. (2.1),

$$\phi(\lambda) = a\lambda^2 + b\lambda + c \tag{2.6}$$

Table 1
Values of λ_m and ρ_m for the four principal Regge poles for the (3,2,0) ← (0,0,0) and (3,3,0) ← (0,0,0) transitions at $E = 0.3872$ and 0.4162 eV. Also given are parameters a, b and c in the quadratic approximation for the phase $\phi(\lambda)$ in Eq. (2.6), lifeangles $\Delta\Theta \equiv (1/2)\mathrm{Im}(\lambda_m)$ and the values of $\gamma \equiv a[\mathrm{Im}(\lambda_m)]^2$

m	Re λ_m	Im λ_m	Re ρ_m	Im ρ_m	γ	$\Delta\Theta$ (deg)
$E = 0.3872$ ev	$v = 0,\ j = 0$	$v' = 3,\ j' = 2$	$a = -7.39\,(-2)$	$b = 2.35\,(-2)$	$c = -3.37\,(-1)$	
1	16.908	0.889	$-3.59\,(-2)$	4.90 (−2)	5.84 (−2)	32.2
2	15.317	2.633	$-1.13\,(-1)$	1.38 (−1)	5.12 (−1)	10.9
3	12.062	2.874	$-3.54\,(-1)$	3.20 (−1)	6.11 (−1)	10.0
4	10.267	3.115	4.07 (−1)	$-7.52\,(-2)$	7.17 (−1)	9.2
$E = 0.4162$ ev	$v = 0,\ j = 0$	$v' = 3,\ j' = 2$	$a = -7.07\,(-2)$	$b = 1.28\,(-1)$	$c = 1.21$	
1	19.136	0.886	$-4.56\,(-2)$	3.92 (−2)	5.54 (−2)	32.3
2	17.167	2.700	5.75 (−2)	1.67 (−1)	5.15 (−1)	10.6
3	14.433	2.403	$-3.54\,(-1)$	$-1.34\,(-1)$	4.08 (−1)	11.9
4	12.091	2.464	1.81 (−3)	4.88 (−2)	4.29 (−1)	11.6
$E = 0.3872$ ev	$v = 0,\ j = 0$	$v' = 3,\ j' = 3$	$a = -6.37\,(-2)$	$b = -1.14\,(-1)$	$c = 1.41$	
1	16.907	0.886	3.31 (−2)	$-6.99\,(-2)$	5.00 (−2)	32.3
2	14.873	3.817	2.34 (−1)	7.97 (−1)	9.27 (−1)	7.5
3	12.349	3.368	1.06	−1.24	7.22 (−1)	8.5
4	10.646	3.496	−0.93	0.19	7.78 (−1)	8.1
$E = 0.4162$ ev	$v = 0,\ j = 0$	$v' = 3,\ j' = 3$	$a = -6.35\,(-2)$	$b = -9.35\,(-2)$	$c = 9.54\,(-1)$	
1	19.139	0.887	$-5.79\,(-2)$	3.41 (−3)	5.00 (−2)	32.3
2	17.223	3.031	1.53 (−1)	$-1.80\,(-1)$	5.83 (−1)	9.5
3	14.855	3.374	$-6.94\,(-1)$	3.96 (−1)	7.23 (−1)	8.5
4	13.635	2.944	3.94 (−1)	$-1.71\,(-1)$	5.50 (−1)	9.6

and identified four resonance poles λ_m ($N_{\mathrm{res}} = 4$). We found it convenient to redefine $\phi(\lambda)$ by adding to it $\mathrm{Arg}[q(\lambda)]$

$$\phi(\lambda) \to \phi(\lambda) + \mathrm{Arg}[q(\lambda)], \tag{2.7}$$

approximate $\phi(\lambda)$ by a quadratic form (2.6) and recalculate the Padé approximation for $s(\lambda)$ in Eq. (2.2). The resulting pole positions λ_m, residues ρ_m and coefficients a, b and c are given in Table 1. Fig. 3a,c show the moduli of $S^J_{\nu' \leftarrow \nu}$ (circles), Padé approximants $S_{\nu' \leftarrow \nu}(\lambda)$ (solid) and smooth terms $q(\lambda)$ (dashed). The derivatives of $\mathrm{Arg}[S_{\nu' \leftarrow \nu}(\lambda)]$ and $\phi(\lambda)$ with respect to λ are shown in Fig. 3b,d by solid and dashed lines, respectively. Also shown by a dot-dashed line is the derivative of the quadratic approximation to $\phi(\lambda)$, $2a\lambda + b$. Next we evaluate the integral in Eq. (1.5).

4. Semiclassical optical model

Collision partners in a chemical reaction are usually sufficiently heavy to justify semiclassical analysis. Thus, we attempt to evaluate the integral (1.5) with a rapidly oscillating term $\exp\{i[\lambda\varphi + \phi(\lambda)]\}$ by the stationary phase method. The stationary phase condition reads

$$\varphi = -\phi'(\lambda_S) = -2a\lambda_S - b \tag{3.1}$$

where prime indicates differentiation with respect to λ. Eq. (3.1) determines the values of the total angular momentum $\hbar\lambda_S$ which classically lead to a precession angle φ. For a single stationary point λ_S, the stationary phase method gives

$$f^{\mathrm{opt}}_{v' \leftarrow v}(\varphi) \approx s_{\nu' \leftarrow \nu}(\lambda_S)\left[\frac{2\pi\lambda_S}{i\phi''(\lambda_S)}\right]^{1/2} \times \exp\{i[\phi(\lambda_S) + \varphi\lambda_S]\}. \tag{3.2}$$

For the transitions (2.5) we have found (Fig. 3b,d)

$$-\pi < \phi'(\lambda) < 0 \tag{3.3}$$

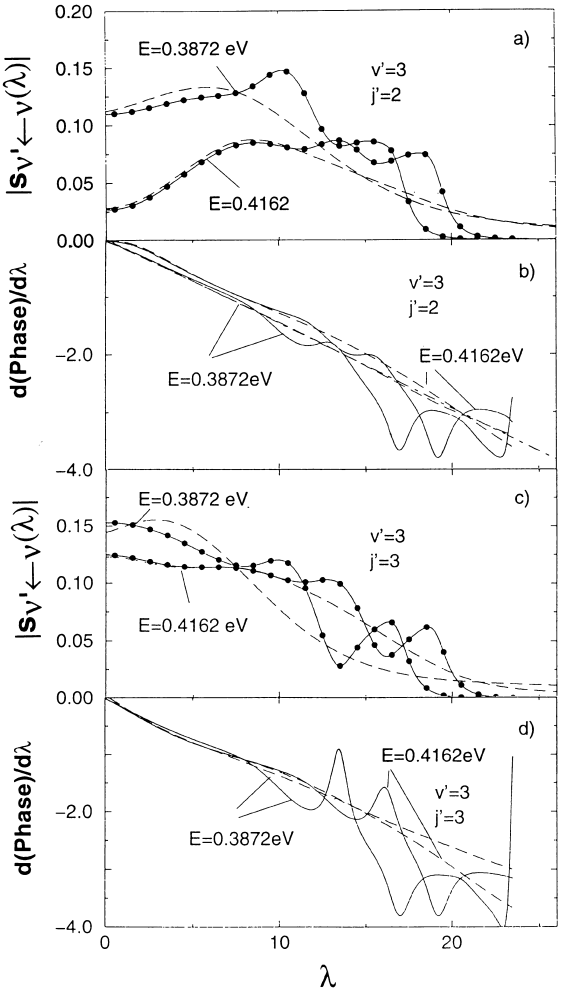

Fig. 3. (a) Transition (3,2,0) ← (0,0,0), moduli of: S-matrix element $S^J = S(J+1/2)$ (circles); Padé approximant $S(\lambda)$ vs. λ (solid); smooth part of the Padé approximant $S(\lambda)$, $q(\lambda)$ (dashed) vs. λ. (b) Transition (3,2,0) ← (0,0,0), derivatives of: the phase of the S-matrix, $\mathrm{dArg}[S(\lambda)]/\mathrm{d}\lambda$, (solid); the phase of the smooth part of the S-matrix, $\mathrm{dArg}[\exp[i\phi(\lambda)]q(\lambda)]/\mathrm{d}\lambda$, (dashed). Also shown by a dot-dashed line is the derivative of the quadratic fit to the smooth phase, $2a\lambda + b$, vs. λ.

so that in Eq. (1.4) only the $k = 0$ (first nearside) term has appreciable magnitude,

$$f^{\mathrm{opt}}_{v'\leftarrow v}(\theta) \approx (ik_v)^{-1}(2\pi\sin\theta)^{-1/2}\,\tilde{f}^{\mathrm{opt}}(\theta)\exp(-i\pi/4) \tag{3.4}$$

where $\tilde{f}^{\mathrm{opt}}(\theta)$ is given by Eq. (3.2).

Our primitive semiclassical approximation (3.4) is similar to the optical model of Herschbach [16,17] in which collision partners are represented by hard spheres of (adjustable) radius R. The classical hard-sphere angular distribution is then modified by the quantum probability for the atom B to be transferred between A and C, $|s_{v'\leftarrow v}(\lambda_S)|^2$ [16,17]. Our optical approximation for the differential cross-section

$$\sigma^{\mathrm{opt}}_{v'\leftarrow v}(\theta) \equiv |f^{\mathrm{opt}}_{v'\leftarrow v}(\theta)|^2 \tag{3.5}$$

yields a similar result but for the classical deflection function

$$\theta(\bar{J}) = -2\hbar^{-1}a\bar{J} - b \tag{3.6}$$

where $\tilde{J} \equiv \hbar\lambda = \hbar(J+1/2)$ is the classical angular momentum. Semiclassical optical angular distributions for the transition (2.5) are shown in Fig. 2 as function of $\theta_R \equiv \pi - \theta$ by dashed lines. The agreement between the exact and optical differential cross-sections is poor, in particular, for small θ_R. This is expected because, for sufficiently large lifeangles, resonance peaks in $S_{v'\leftarrow v}(\lambda)$ are destroyed by rotation and replaced in $f_{v'\leftarrow v}(\theta)$ by exponentially decaying tails [7,8]. Next we correct the model to account for this effect.

5. Lifetime correction function

Mathematically, the optical model (3.2)–(3.4) fails because the primitive semiclassical approximation of Section 4 breaks down when the stationary point λ_S approaches one of the poles λ_m, $m = 1,2\ldots N_{\mathrm{res}}$. To obtain a uniform approximation for $\tilde{f}_{v'\leftarrow v}(\varphi)$, we first subtract $\sum_{m=1}^{N_{\mathrm{res}}}\lambda_m^{1/2}\rho_m\exp[i\lambda\varphi + i\phi(\lambda)](\lambda - \lambda_m)^{-1}$ from the integrand of Eq. (1.5). The resulting integral has no poles at $\lambda = \lambda_m$ and can be evaluated by the method of Section 4. In the remaining integrals containing pole contributions $\lambda_m^{1/2}\rho_m\exp[i\lambda\varphi + i\phi(\lambda)](\lambda - \lambda_m)^{-1}$ we replace the lower integration limit by $-\infty$, and express them in terms of the complementary error functions (see Appendix A). The result can be written as

$$\tilde{f}_{v'\leftarrow v}(\varphi) = \tilde{f}^{\mathrm{opt}}_{v'\leftarrow v}(\varphi) + \delta\tilde{f}_{v'\leftarrow v}(\varphi)\,. \tag{4.1}$$

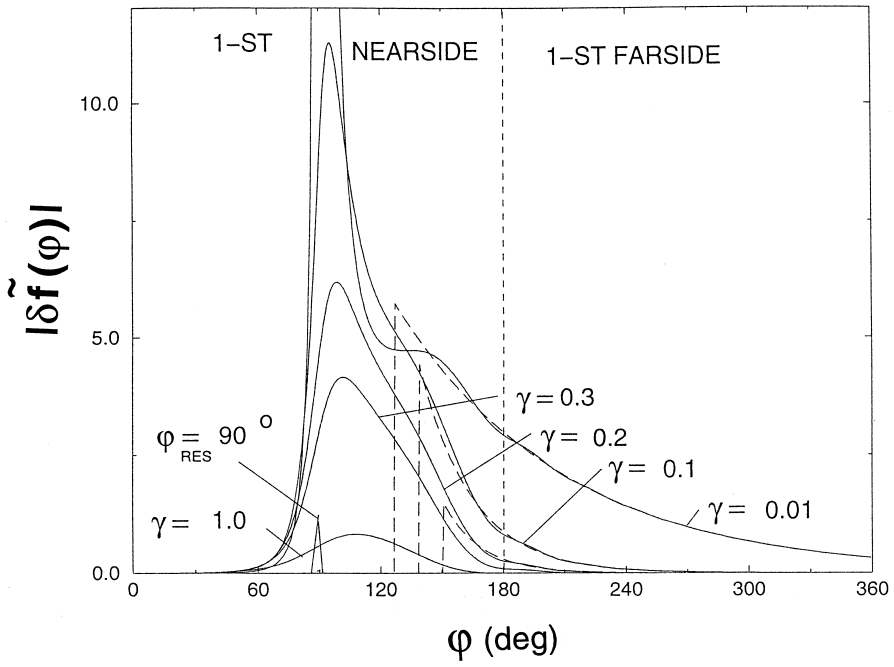

Fig. 4. The LCF $\delta\tilde{f}(\varphi)$ for a single pole λ_0 with $\varphi_{res} = 90°$, $a = -0.08$ for different values of $\gamma \equiv a[\mathrm{Im}\,\lambda_0]^2$, $\gamma = 0.01, 0.1, 0.2, 0.3, 1.0$. Also shown by dashed lines is the exponential asymptote in (4.9). The exponential tail is drawn where the error of (4.12) is less than 10%.

where

$$\delta\tilde{f}_{\nu'\leftarrow\nu}(\varphi) = \sum_{m=1}^{N_{res}} \delta\tilde{f}^{m}_{\nu'\leftarrow\nu}(\varphi)\,, \tag{4.2}$$

and

$$\delta\tilde{f}^{m}_{\nu'\leftarrow\nu}(\varphi) = \lambda_m^{1/2}\rho_m\Big\{ i\pi\exp\{i[\Phi(\lambda_m)]\} \times \mathrm{erfc}\big[(-ia)^{1/2}(\lambda_m - \lambda_S)\big] - \frac{1}{\lambda_S - \lambda_m}\left[\frac{2\pi}{-\Phi''(\lambda_S)}\right]^{1/2} \times \exp\{i[\Phi(\lambda_S)]\}\Big\}. \tag{4.3}$$

Also,

$$\Phi(\lambda) = a\lambda^2 + (b+\varphi)\lambda + c\,, \tag{4.4}$$

$$\lambda_S(\varphi) = -(\varphi + b)/2a\,, \tag{4.5}$$

and

$$\mathrm{erfc}(z) \equiv \frac{2}{\pi^{1/2}}\int_z^{\infty}\exp(-t^2)\,\mathrm{d}t \tag{4.6}$$

is the complementary error function [18].

Eqs. (4.1), (4.2) and (4.3), which are exact to semiclassical accuracy, are our main result for a system which, like $F + H_2$, has a quadratic phase (2.6). The first term in Eq. (4.1) corresponds to the optical model of Section 4, while the second one contains corrections due to the finite lifetimes (lifeangles) of the resonances. If the resonances are too short-lived for the complexes to rotate before decaying into products $\delta\tilde{f}_{\nu'\leftarrow\nu}(\varphi)$ vanishes and the optical model result is recovered. If some of the lifeangles are large, the full scattering amplitude can be seen as a result of interference between $\tilde{f}^{opt}_{\nu'\leftarrow\nu}$ and several correction terms.

For each pole term, the lifetime correction function (LCF) $\delta\tilde{f}^{m}_{\nu'\leftarrow\nu}(\varphi)$ (4.3) is the difference between the uniform (error function) result and the primitive semiclassical approximation of Section 4.

Consider its behaviour as a function of Im λ_m. Let $\varphi_{\rm res} \equiv (a\,{\rm Re}\,\lambda_m + b)$ be the direct scattering angle corresponding to $\lambda = {\rm Re}\,\lambda_m$. Using well-known properties of the error function [18],

$$
\begin{aligned}
&{\rm erfc}(z) \approx (\pi^{1/2} z)^{-1} \exp(-z^2)\,,\\
&|z| \to \infty,\ |{\rm Arg}\, z| < \pi/2\,,\\
&{\rm erfc}(-z) = 2 - {\rm erfc}(z)\,, \qquad (4.7)
\end{aligned}
$$

we find that for $\varphi \ll \varphi_{\rm res}$

$$
\delta \tilde{f}^{m}_{v' \leftarrow v}(\varphi) \approx 0\,. \qquad (4.8)
$$

For $\varphi \gg \varphi_{\rm res}$ the LCF describes rotation and decay of the complex, and has a simple exponential form

$$
\begin{aligned}
\delta \tilde{f}^{m}_{v' \leftarrow v}(\varphi) &\approx 2\pi i \rho_m \exp\{i\Phi(\lambda_m)\}\\
&\approx {\rm const} \times \exp\{i\varphi({\rm Re}\,\lambda_m + i\,{\rm Im}\,\lambda_m)\}\,. \qquad (4.9)
\end{aligned}
$$

Around $\varphi \approx \varphi_{\rm res}$ we have a *transitional region* $\Delta\varphi$ where direct scattering cannot be distinguished from immediate decay of a newly formed complex. A long-lived state is formed if λ lies in the range $\Delta\lambda \approx {\rm Im}\,\lambda_0$ around Re λ_m. The width of the corresponding direct angular range gives the size of the transitional region, $\Delta\varphi \approx \Phi''({\rm Re}\,\lambda_m)$, $\Delta\lambda \approx a({\rm Im}\,\lambda_m)$. As Im $\lambda_m \to 0$, we find $\Delta\varphi \approx a \approx \hbar$ (note that as $\hbar \to 0$ we must have $a \approx \hbar$ for the classical deflection function (3.6) to have a finite slope) and the LCF sharply peaked in the transitional region. As the pole moves away from the real axis, its exponential tail (4.9) becomes shorter, while $\Delta\lambda$ grows. At the same time the magnitude of the LCF decreases as $\tilde{f}_{v' \leftarrow v}(\varphi)$ tends to $\tilde{f}^{\rm opt}_{v' \leftarrow v}(\varphi)$. The condition for a resonance to produce a distinct exponential contribution to $\tilde{f}_{v' \leftarrow v}(\varphi)$ requires $1/{\rm Im}\,\lambda_m \gg \Delta\varphi$, or, equivalently,

$$
\gamma \equiv a[{\rm Im}\,\lambda_m]^2 \ll 1\,.
$$

The LCF for a (fictitious) pole λ_0 with $\varphi_{\rm res} = 90°$, $\rho_0 = 1$, $a = -0.08$ and $b = c = 0$ is shown in Fig. 4 for $\gamma = 0.01$, 0.1, 0.2, 0.3, 1.0. Note that a well-defined exponential tail disappears already at $\gamma \approx 0.3$. Next we apply the method to the title reaction.

6. Analysis of $F + H_2$ angular scattering

For the two transitions (2.5) and two energies (0.3282 and 0.4162 eV), we find that $\tilde{f}_{v' \leftarrow v}(\varphi)$ is well extended into the first farside region $180° < \varphi < 360°$ and has almost no structure (Fig. 5). The optical model result $\tilde{f}^{\rm opt}_{v' \leftarrow v}$, shown in Fig. 5 by a dot-dashed line, is contained in the (first nearside)

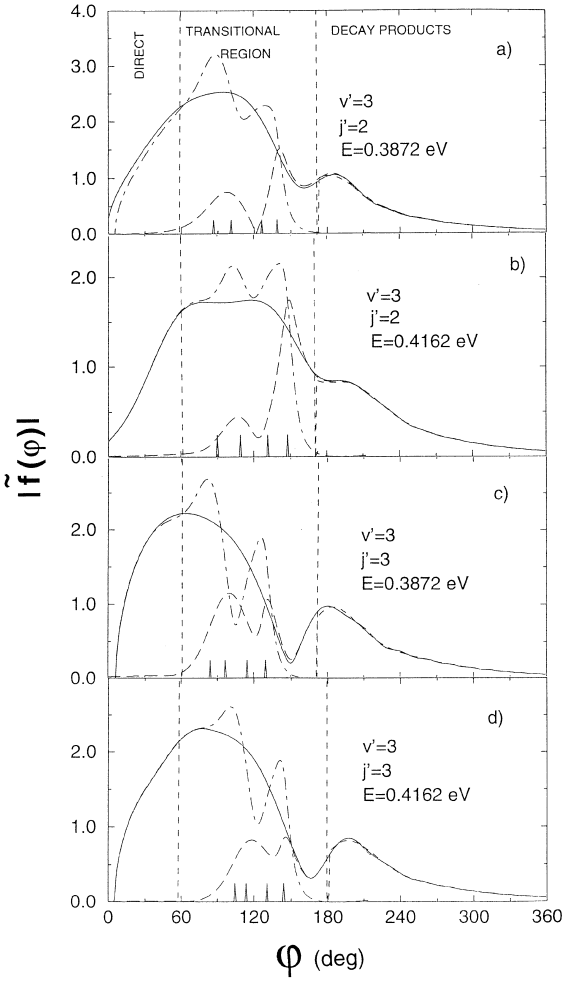

Fig. 5. (a) Transition (3,2,0) ← (0,0,0) at $E = 0.3872$ eV: the optical model result $\tilde{f}^{\rm opt}(\varphi)$ (dot-dashed), the LCF $\delta\tilde{f}(\varphi)$ which includes the four poles in Table 1 (long dashed) and the full semiclassical amplitude $\tilde{f}(\varphi) = \tilde{f}^{\rm opt}(\varphi) + \delta\tilde{f}\varphi$. Also shown are the resonance angles $\varphi_{\rm res}$ for the four poles (spikes) and the exponential tail (4.9) (dashed). (b) Same as (a) but for $E = 0.4162$ eV. (c) Same as (a) but for the (3,2,0) ← (0,0,0) transition. (d) Same as (c) but for $E = 0.4162$ eV.

region $0° < \varphi < 180°$. In all cases, the four-pole LCF shown in Fig. 5 by a dashed line has a transitional region at $60° < \varphi < 180°$ and for $\varphi < 60°$ all scattering is direct. In the first farside region, $\delta\tilde{f}_{\nu' \leftarrow \nu}(\varphi)$ has an exponential tail which can be attributed to the decay of a single Regge state, $\lambda_1 \approx 16.91 + i0.89$ at $E = 0.3872$ eV and $\lambda_1 \approx 19.14 + i0.89$ at $E = 0.4162$ eV (Table 1).

The forward scattering and nearside–farside oscillations observed in Ref. [4] (Fig. 2, solid), should therefore be interpreted as a resonance effect. Our semiclassical model (Fig. 2, dot-dashed) reproduces these oscillations to almost graphical accuracy. Finally, note that although only the leading $(m = 1)$ resonance has a considerable angular life $(\gamma \approx 0.06)$ we need, in general, all four poles to achieve a good agreement between exact and semiclassical cross-sections. Semiclassical results with only the leading pole included in the LCF are shown in Fig. 2 by a long-dashed line.

7. Summary and conclusions

We have developed a simple method to estimate resonance effects in reactive (also in elastic and inelastic) atom–diatom angular distributions. Introduction of the amplitude $\tilde{f}_{\nu' \leftarrow \nu}(\varphi)$ allows us 'unfold' the scattering amplitude $f_{\nu' \leftarrow \nu}(\theta)$ by separating different rotations of the Jacobi vector $\boldsymbol{R}_{\mathrm{BC} \to \mathrm{A}}$ around the total angular momentum. Semiclassically, $\tilde{f}_{\nu' \leftarrow \nu}(\varphi)$ is decomposed into the direct and resonance contributions (except in the transitional region, where such decomposition is not possible). A structure in the angular distribution can then be explained as a result of interference between various direct, resonance, nearside and farside contributions. The Padé method has been used to accurately obtain the positions and residues of the resonance poles.

For the two $\mathrm{F} + \mathrm{H}_2 \to \mathrm{FH} + \mathrm{H}$ transitions (2.5) we attribute the small angle scattering as well as the nearside–farside oscillations to the decay of the Regge state corresponding to the leading pole. This agrees with the finding of Dobbyn et al. [5]. Note, however, that a direct comparison with the conclusions of Ref. [4] requires analysis of cross-sections summed over all helicity and rotational quantum numbers. We intend to do this in future work.

Acknowledgements

One of us (D.S.) is grateful to Professor D. Bessis for introduction to the Padé method, to Dr. A.J. Dobbyn for useful discussions and to Professor J.N.L. Connor for helpful discussions and hospitality during a visit to Manchester.

Appendix A

Consider an integral of the form

$$I \equiv \int_{-\infty}^{\infty} \frac{\exp(A\lambda^2 + B\lambda)}{\lambda - \lambda_0}\,\mathrm{d}\lambda, \quad \mathrm{Im}\,\lambda_0 > 0. \qquad (A.1)$$

For $\mathrm{Im}\,\lambda_0 > 0$ we can rewrite (A.1) as

$$I \equiv -\int_{-\infty}^{\infty} \mathrm{d}\lambda \int_0^{\infty} \mathrm{d}t \exp\left[A\lambda^2 + B\lambda + t(\lambda - \lambda_0)\right]. \qquad (A.2)$$

Evaluation of the Gaussian integral over λ gives

$$I = i(\pi/A)^{1/2} \int_0^{\infty} \mathrm{d}t \exp\left[-(B+t)^2/4A - t\lambda_0\right]. \qquad (A.3)$$

Finally, a change of variables $t \to (t + B)/(2\sqrt{A}) + \sqrt{A\lambda_0}$ yields

$$I = i\pi \exp\left[A\lambda_0^2 + B\lambda_0\right] \mathrm{erfc}\left(B/\left(2\sqrt{A}\right) + \sqrt{A\lambda_0}\right)$$

where $\mathrm{erfc}(z)$ is the complementary error function [18] in Eq. (4.7). Choosing $A = a$, $B = (b \pm \theta + 2\pi n)$ and $\lambda_0 = \lambda_m$, we obtain the first term in Eq. (4.3).

References

[1] D.M. Neumark, A.M. Wodtke, G.N. Robinson, C.C. Hayden, Y.T. Lee, J. Chem. Phys. 82 (1985) 3045.
[2] F.J. Aoiz, L. Bañnares, V.J. Herrero, V. Sa'ez Ra'banos, K. Stark, H.-J. Werner, J. Chem. Phys. 102 (1995) 9248.
[3] J.F. Castillo, D.E. Manolopoulos, K. Stark, H.-J. Werner, J. Chem. Phys. 104 (1996) 6531.
[4] J.F. Castillo, B. Harthe, H.-J. Werner, F.J. Aoiz, L. Bañares, B. Martinez-Haya, J. Chem. Phys. 109 (1998) 7224.
[5] A.J. Dobbyn, P. McCabe, J.N.L. Connor, J.F. Castillo, Phys. Chem. Chem. Phys. 1 (1999) 1115.

[6] J.N.L. Connor, P. McCabe, D. Sokolovski, G.C. Schatz, Chem. Phys. Lett. 206 (1993) 119.
[7] D. Sokolovski, J.N.L. Connor, G.C. Schatz, Chem. Phys. Lett. 238 (1995) 127.
[8] D. Sokolovski, J.N.L. Connor, G.C. Schatz, J. Chem. Phys. 103 (1995) 5979.
[9] W.H. Miller, J. Chem. Phys. 53 (1970) 1949.
[10] G.C. Schatz, A. Kupperman, J. Chem. Phys. 65 (1976) 4642.
[11] D.M. Brink, G.R. Satcher, Angular Momentum, Clarendon Press, Oxford, 1962.
[12] D.M. Brink, Semiclassical Methods for Nucleous–Nucleous Scattering, Cambridge University, Cambridge, 1992.
[13] D. Sokolovski, J.N.L. Connor, Chem. Phys. Lett. 305 (1999) 238.
[14] G.A. Baker, Jr., The Essentials of Padé Approximations, Academic, New York, 1975.
[15] D. Bessis, A. Haffad, A.Z. Msezane, Phys. Rev. A 49 (1994) 3366.
[16] D.R. Herschbach, Appl. Opt. 2 (1965) 128, Suppl.
[17] D.R. Herschbach, Adv. Chem. Phys. 10 (1966) 319.
[18] W. Gautschi, in: M. Abramowitz, I.A. Stegun, Handbook of Mathematical Functions, National Buro of Standards, Applied Mathematics Series, 1964.